

Influence of the pressure dependent coefficient of friction on deep drawing springback predictions

Imanol Gil^{1*}, Joseba Mendiguren¹, Lander Galdos¹, Endika Mugarra¹, Eneko Saenz de Argandoña¹

¹ Department of Mechanical and Industrial Production, Mondragon Unibertsitatea, Loramendi 4, Mondragon 20500, Gipuzkoa, Spain

*Corresponding author. Email: igil@mondragon.edu

Abstract

The aim of this work is to show the influence of defining a pressure dependent friction coefficient on numerical springback predictions of a DX54D mild steel, a HSLA380 and a DP780 high strength steel. The pressure dependent friction model of each material was fitted to the experimental data obtained by Strip Drawing tests and then implemented in the numerical simulation of an industrial automotive part drawing process. The results showed important differences between defining a pressure dependent or a constant friction coefficient. Finally, the experimental part was produced to compare the real geometry with the predictions obtained with the different simulation strategies. An improvement of 20-25% in springback prediction was achieved when using the pressure dependent friction model.

Keywords: Springback; friction; Strip Drawing test; high strength steel

1 Introduction

The automotive industry demands very short delivery periods. This leaves no margin for errors that could prolong the time that die suppliers have to fulfill the requirements of their clients. Accurate die designs reduce the need for subsequent redesigns, thereby decreasing time and manufacturing costs. Current design procedures are based on numerical simulations that predict the behavior of sheet metal parts with the aim of achieving more efficient manufacturing processes.

Furthermore, in the assembly lines of the automotive industry most of the joints between components are handled by automatic robotic arms. This requires geometric tolerances to be increasingly strict. For this reason, the springback phenomenon is of great importance. Springback is defined as the elastic recovery that the part suffers after being deformed to a determined shape. The accurate prediction of springback is one of the biggest issues in stamping and a lot of research has been done in this topic in recent years [1]. Previous works state that the use of kinematic hardening models [2], advanced anisotropy constitutive models [3] and Young modulus degradation models [4] significantly increases the accuracy of the numerical springback prediction. Apart from the material parameters, springback is mainly influenced by the meshing quality of the numerical simulation [5] and the coefficient of friction (COF) definition [6].

In a deep drawing operation, three main tools are involved: the punch, the die and the blankholder. In these dies two areas can be distinguished; the die cavity area, where the sheet is deformed to the required shape of the part, and the blankholder area, where the flow of the material is restricted. In this area, the drawbeads in combination with the friction forces determine the restriction forces that the material has to overcome to flow into the die cavity. By this way, the draw-in of the material is controlled and in consequence the strain and stress distribution of the sheet. So the COF is critical in the blankholder area as it is the zone where the maximum flow of the material occurs.

The COF is a significant parameter to take into account when trying to obtain accurate predictions in numerical simulation [7]. As it is explained in the previous paragraph, the COF influences the restriction level of the material flow through the tools and an inaccurate definition of the parameter generates wrong predictions such as splits, insufficient deformations and, moreover, unexpected springback phenomena. A lower COF induces lower stress-states and as a consequence higher elastic recovery [6]. Therefore, it is necessary to correctly define the COF in order to accurately predict the final geometry of the component through the numerical simulation.

Traditionally, the COF has been considered to remain constant during the drawing process of a component. However, some studies discussed the possibility of applying different constant COF for each surface that is in contact with the sheet [8]. More recent tribological studies have revealed that the COF is affected by several contact features. In this way some authors have developed variable COF models based on micro-scale contact behavior [9,10] or macro-scale [11,12] ones. In both cases there is a generalized agreement that one of the most important parameter affecting the COF is the contact pressure [13]. As the contact pressure is increased, the irregular topography of the contact surfaces are subjected to a flattening of each asperities, so the contact geometry changes resulting in a change of the COF [14]. This is an important effect to take into account since in drawing processes, the blankholding force remains constant but the contact pressure applied to the sheet increases as the flange area decreases while the material flows into the die cavity. Moreover, the thickness changes differently in each area of the sheet with the flow of the material causing a heterogeneous contact pressure distribution along the sheet. Therefore, the contact pressure varies continuously during the drawing.

Asgari et al. [15] studied the influence of the coefficient of friction on an industrial B-Pillar automotive part and concluded that it was not relevant for the springback prediction. Other researchers disagreed and demonstrated that the COF has a great importance on the prediction of the springback [16]. In terms of the robustness of springback predictions Souza et al. [17] determined that springback results are more sensitive to high friction values than to low ones. Lee et al. [18] have also recently studied the influence of implementing a variable COF on the springback prediction of a U-bending test. However, it has not been analyzed yet the effect of a variable COF on a real industrial component where the contact pressure is not homogeneous on the blankholding area.

In this work, the effect of a pressure dependent COF model in the springback prediction of an industrial component is analyzed. For that, the effect of three friction models, two models with constant friction values and one pressure dependent model were compared. In order to characterize the COF behavior on the blankholder area, Strip drawing tests at

different pressure values, ranging from 1 MPa to 16 MPa, were carried out and then a pressure dependent model was fitted to the experimental results. The effect of each friction model was numerically analyzed on a B-Pillar reinforcement component using three different steel grades: a DX54D mild steel (0.7 mm thickness), a HSLA380 (1.05 mm thickness) and a DP780 high strength steel (1.3 mm thickness). Finally, the numerical results were compared to the geometry of a manufactured B-Pillar reinforcement in order to determine the most promising model in terms of springback prediction accuracy.

2 Mechanical characterization

The materials studied in this work were characterized following the ASTM E8-04 standard tensile tests. The selected materials cover a wide range of strength from a mild steel of around 150 MPa of yield strength up to a high strength steel of about 500 MPa of yield strength (Figure 1). These results were used for the material definition in the numerical simulation.

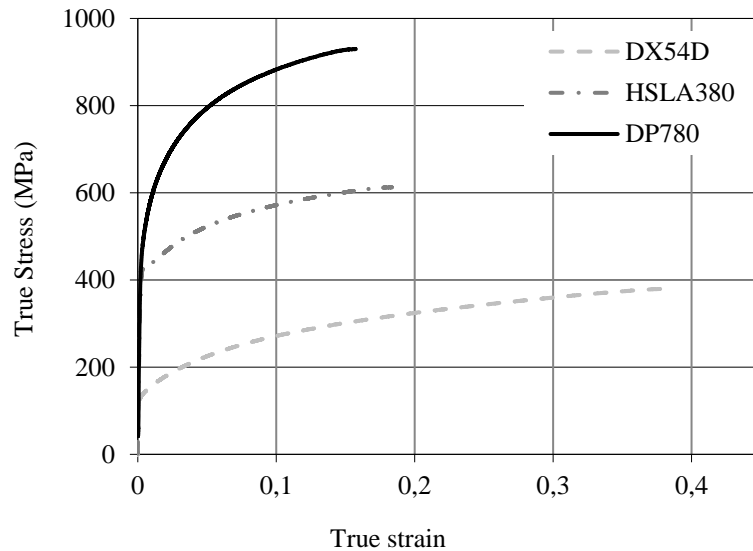


Figure 1 – Tensile test curves of the three materials studied in rolling direction

In Table 1 the summary of the most important parameters of the materials is shown. As it can be seen, the DX54D and DP780 are coated by hot dip galvanized, while the HSLA380 is a non-coated sheet.

Table 1 – Strength of steels, uniform elongation, r-value, roughness, thickness and steel type

Material	Rp0.2 (MPa) Yield Strength	Rm (MPa) Ultimate Tensile Strength	Ag (%) Uniform elongation	$r_0 / r_{45} / r_{90}$	Roughness (Ra)	Thickness (mm)	Steel type and surface coating
DX54D	153	309	27.8	1.87 / 1.75 / 1.56	1.33	0.7	Mild Steel hot dip galvanized
HSLA380	439	519	23.7	0.76 / 1.14 / 0.77	1.51	1.05	High Strength Low Alloy no coating

DP780	490	786	12.6	0.76 / 0.89 / 0.82	1.19	1.33	Dual Phase hot dip galvannealed
-------	-----	-----	------	-----------------------	------	------	---------------------------------------

3 Friction characterization

The friction characterization was carried out using the Strip Drawing test [13]. The tests were conducted using a biaxial testing machine of 4 independent 25 Ton hydraulic cylinders. One of the cylinders made the clamping force while the other cylinder pulled the sheet tangentially to the surface of the blocks, as set out in Figure 2.

The cadency of the deep drawing of the component was about 10 strokes per minute. Since the maximum draw-in was 36 mm the Strip Drawing tests were carried out in a constant velocity of 10 mm/s. The tests were performed at contact pressures ranging from 1 to 16 MPa and using pre-lubricated sheets by MULTIDRAW PL 61 SE (1.5 g/m²) without any additional lubrication.

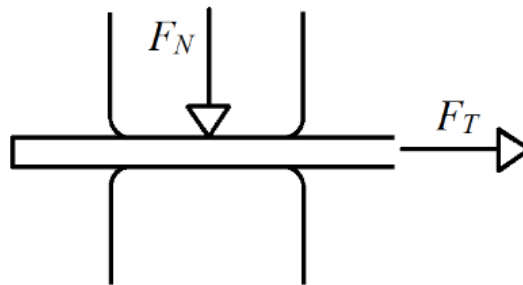


Figure 2 – Schematic representation of a Strip Drawing test

The pressure range was defined in concordance with the observed contact pressures at the blankholding area in the numerical simulations. Figure 3 shows the contact pressure distribution along the sheet. As it can be seen, the major sheet area is under low contact pressures. However, due to the local thickening of the sheet on some blankholding areas, the contact pressure arises up to 16.7 MPa at a determined moment of the process.

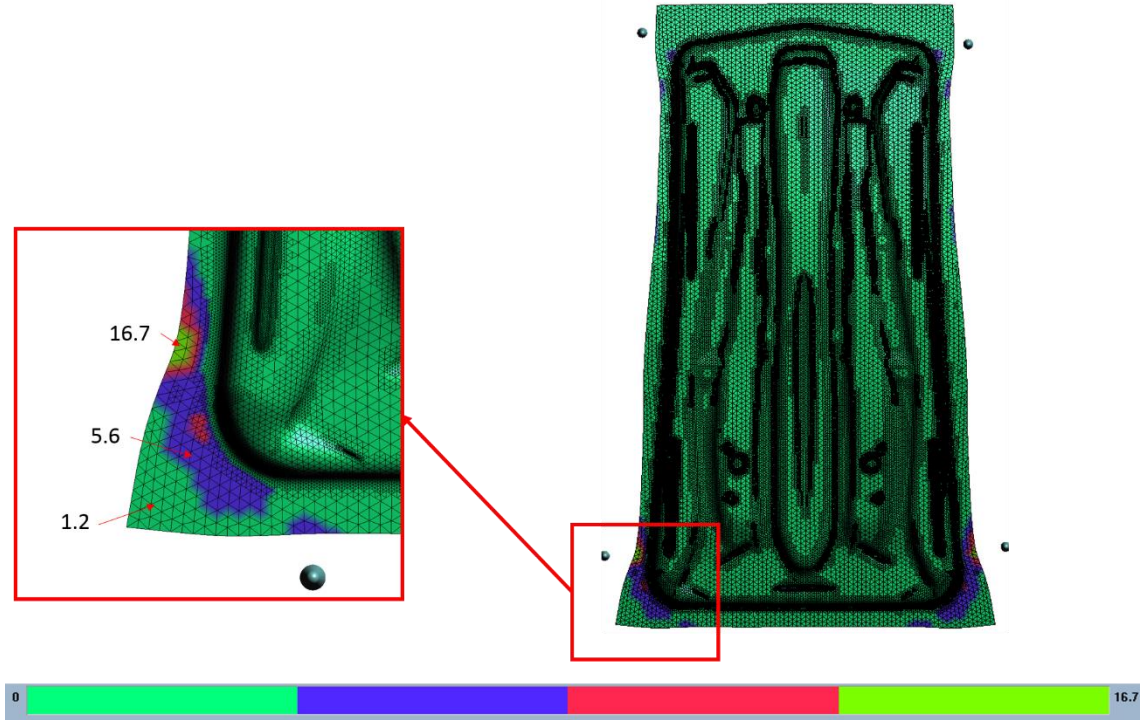


Figure 3 – Contact pressure distribution along the sheet in the numerical simulation of the B-Pillar reinforcement

The material and the surface roughness of the blocks used in the Strip Drawing tests were the same as the ones used in the die and the binder of the experimental drawing process. The blocks were manufactured using a GGG70 tempered grey iron and the surface roughness was about $0.4 \mu\text{m}$ achieved through industrial standard polishing procedure. The contact surface was 52 mm length and 26 mm wide.

The COF value was obtained from the existing relation between the clamping force, F_N , and the tangential force, F_T , presented in the next equation,

$$\mu = \frac{F_T}{2F_N}. \quad (1)$$

The model chosen to represent the tribological behavior of the materials was introduced by Filzek [12] as,

$$\mu = \mu_0 \left(\frac{p}{p_0} \right)^{n-1} \quad (2)$$

where μ_0 and p_0 are reference values and n is an exponent defined within the range $0 < n < 1$. Figure 4 shows the evolution of the COF of each material for the range of contact pressures.

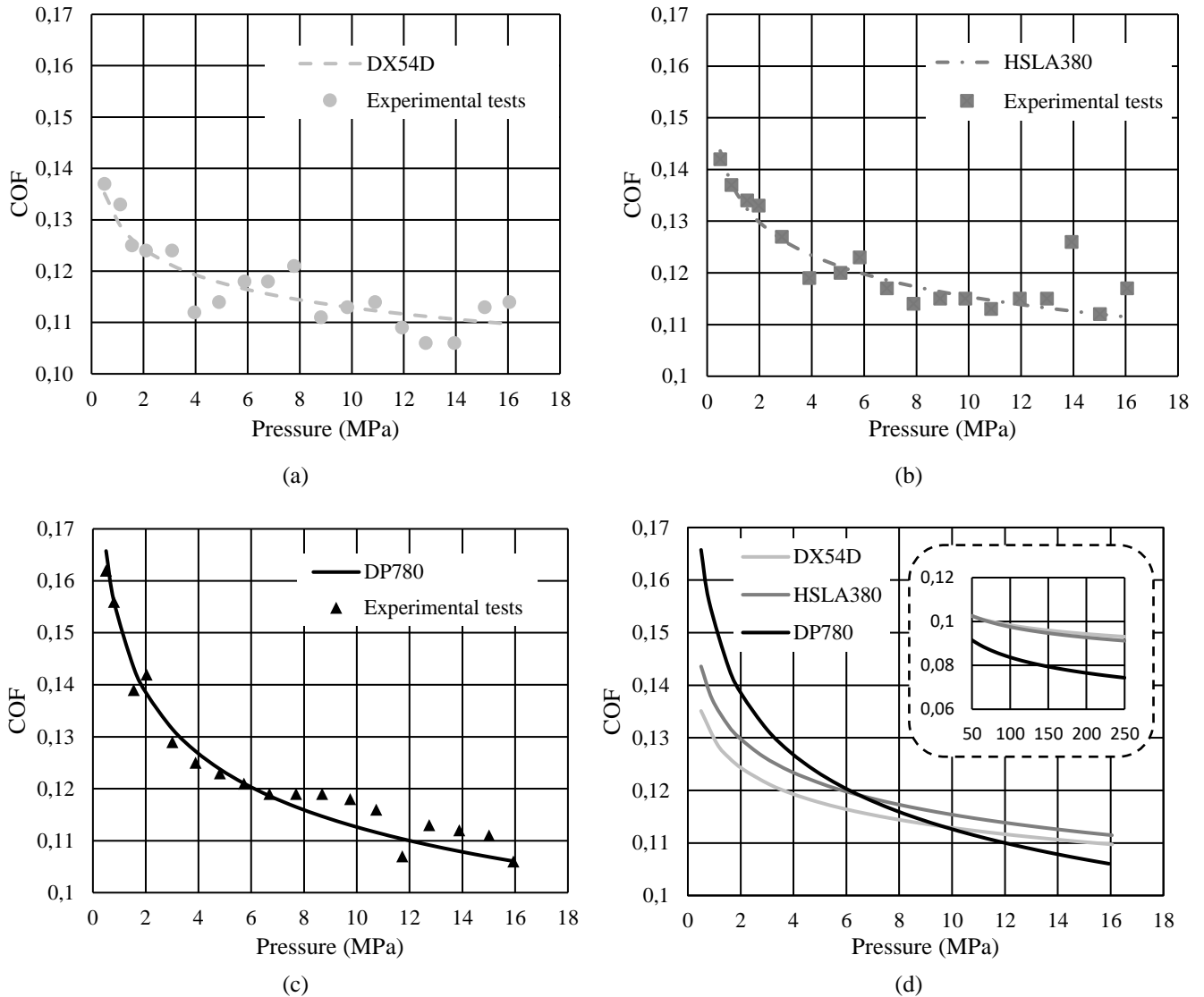


Figure 4 – COF value at different contact pressures. Markers represent the experimental values and lines represent the fitted friction models: (a) DX54D, (b) HSLA380, (c) DP780 and (d) a summary of all the materials

It can be seen that the COF value decreases as the contact pressure increases in every material. This tendency is more evident in the contact pressure range from 1 MPa to 4 MPa. Previous authors studied this phenomenon and concluded that the surface deformation was a predominant effect on the COF evolution at lower contact pressures leading to significant changes of the COF at those pressures [19].

Figure 4 shows a 30% reduction in the COF in the high strength steel DP780 while the difference in the DX54D mild steel is only about 15% for the same range of 1 MPa to 16 MPa of testing pressures. The average COF values and the range of the obtained results for each material are presented in Table 2.

Table 2 – Average, maximum and minimum COF values of the experimental result obtained in the strip drawing tests

Material	Average COF ($\bar{\mu}$)	Maximum COF (μ_{\max})	Minimum COF (μ_{\min})
DX54D	0.116	0.133	0.106
HSLA380	0.121	0.137	0.112
DP780	0.120	0.156	0.106

It can be observed that the average COF value is quite similar, around 0.12. However, there are differences in terms of variation between materials. The DP780 shows almost twice the variation compared to the DX54D and the HSLA380.

Three different COF evolution models have been used in this work:

- a) A constant COF 0.15 value model (commonly used industrial standard COF)
- b) A constant COF model where the average value of each experimental data (Fig.4) is taken
- c) A pressure dependent COF following Filzek's model (Eq.2)

In order to evaluate the accuracy of each model to represent the measured experimental data, an average relative error, \bar{E} , and the maximum relative error, E_{max} , have been calculated following

$$\bar{E} = \frac{\sum_{i=1}^n \frac{\mu_{\text{exp}_i}(P) - \mu_i(P)}{\mu_{\text{exp}_i}(P)} \cdot 100}{n}, \quad (3)$$

where $\mu_{\text{exp}_i}(P)$ is the experimentally obtained data, $\mu_i(P)$ is the calculated COF and n is the number of data points.

Table 3 – Average errors of different COF models with experimentally obtained values

Material	\bar{E} / E_{max} , Pressure dependent (%)	\bar{E} / E_{max} , Average COF (%)	\bar{E} / E_{max} , COF=0.15 (%)
DX54D	2.8 / 6.6	6.1 / 13.2	29.6 / 41.5
HSLA380	2.2 / 10.6	5.1 / 12.4	24.8 / 33.9
DP780	2.2 / 4.2	7.1 / 23.1	24.6 / 41.5

These results show the reduction in error from 25% to 2.5% when representing the COF as pressure dependent. In the same way, a reduction from about 25% to 6% is obtained when representing the COF as a constant value but with the averaged value obtained from the experimental tests (Figure 4).

4 Numerical simulation

In order to evaluate the springback prediction of an industrial component, a B-Pillar reinforcement was chosen. This component was already used in previous researches that studied the springback prediction and posterior compensation of the tools geometry [20].

AUTOFORM R3.1 finite element software was used to simulate both the forming and the springback processes in this study. In order to have the most reliable numerical simulation, intermediate springback operations were defined to reproduce a real multi-operations process.

All simulations were defined with a sheet thickness of 1.05 mm with elastic plastic shell elements, an initial element size of 10 mm with a maximum of 4 refinement levels and 11 layers through the thickness. The three COF values described before were applied for

the simulation of each material. Two constant values, 0.15 and the average COF value obtained in the friction characterization, and the pressure dependent COF model fitted for each material. The pressure dependent COF model has been implemented by the Filzek's model and the parameters used for each material are shown in Table 4.

Table 4 – Pressure dependent COF model's parameters of each material

Material	n	p_0 (MPa)	μ_0
DX54D	0.940	1.946	0.125
HSLA380	0.927	1.857	0.130
DP780	0.871	0.996	0.152

The mechanical behavior of the three steels was defined to be elastoplastic. The elastic behavior is isotropic and constant, with $E = 210$ GPa and $\nu = 0.30$. The Hill'48 yield criterion was used to describe the anisotropic behavior of the three steels, using the Lankford coefficients (r_0, r_{45}, r_{90}) obtained experimentally for each material, see Table 1. The materials hardening models were defined by the isotropic hardening model Combined Swift-Hockett Sherby. This isotropic work hardening law describes the flow stress with plastic work as

$$\sigma = (1 - \alpha) \left(C (\varepsilon_{pl} + \varepsilon_0)^m \right) + \alpha \left(\sigma_S - (\sigma_S - \sigma_Y) e^{-a \varepsilon_{pl}^p} \right), \quad (4)$$

where σ is the flow stress, α is the combination factor, ε_{pl} is the true plastic deformation, ε_0 is the initial elastic deformation, σ_S is the saturation stress, σ_Y is the yield stress, a and m are the work hardening exponents and C and p are material constants. The parameters used for the hardening model of each material, shown in Table 5, were fitted from the tensile test results. For the simulation of sheet metal forming, constitutive modelling based on non-isotropic hardening models, unloading elastic modulus and non-quadratic yield criterion have been proved to be more accurate than classical models [3]. In this case, these observations were not taken into account as the goal of this work is to show the influence of the pressure dependent coefficient of friction independently to other process or material variables.

Table 5 – Constitutive hardening model parameters of the three materials

Material	α	ε_0	σ_S (MPa)	σ_Y (MPa)	a	m	C (MPa)	p
DX54D	0.25	0.0016	363.4	160.4	13.6	0.201	537.0	0.823
HSLA380	0.25	0.0203	647.4	438.9	8.54	0.152	793.5	0.905
DP780	0.25	0.0026	939.2	488.1	6.43	0.142	1135.8	0.676

The simulation was defined by different operations as seen in Figure 5. The operations chain is as follows: Drawing \rightarrow Springback (free) \rightarrow Trimming \rightarrow Springback (free) \rightarrow Trimming \rightarrow Springback (free) \rightarrow Forming \rightarrow Cutting \rightarrow Springback (constrained).

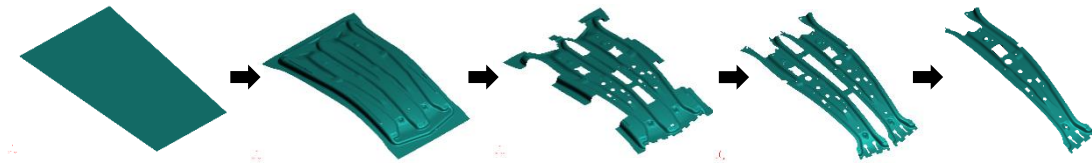


Figure 5 – Numerical model process sheet forming sequence

The final springback was constrained as set out in Figure 6. Two pilots and four one-side clamps were used to locate the part and to measure the elastic recovery. The pilots and the clamps were defined based on the clamping device used to experimentally digitalize the component.

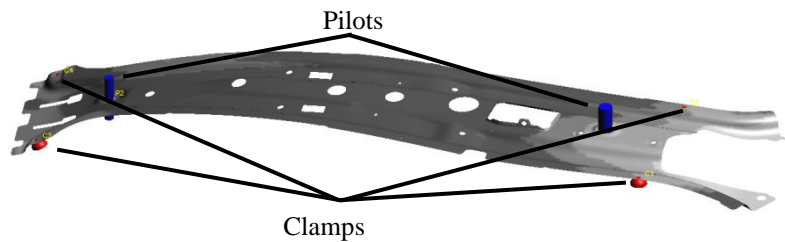


Figure 6 – Constraining supports

5 Experimental work

In addition to the numerical comparison to show the differences between the COF models, an experimental work was carried out to identify the most accurate COF model. The experiments were performed in a mechanical single action press of 20000 kN with a ram velocity of around 200 mm/s. As in the simulation, a 1600 kN blankholder force was applied and drawbeads were used to control the flow of the material through the tools. The sheets were pre-lubricated by MULTIDRAW PL 61 SE (1.5 g/m²) without any additional lubrication.

The high strength HSLA380 steel was used as benchmark material for the experimental validation (Figure 7). After the forming, the sheet was clamped in a reference fixture and then measured by a commercial digital measuring device.

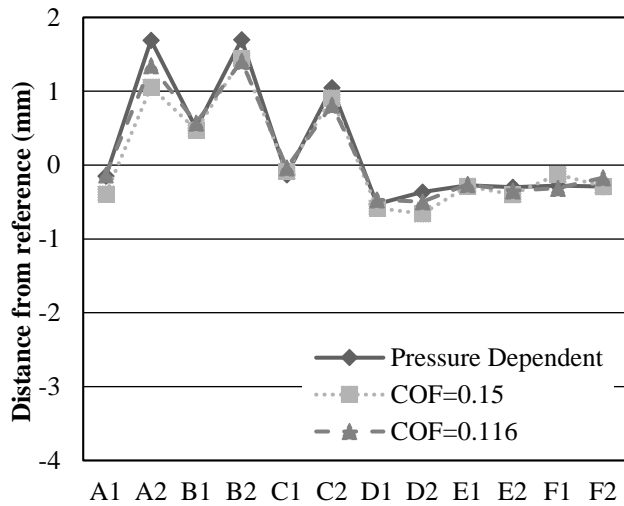


Figure 7 – Drawn part

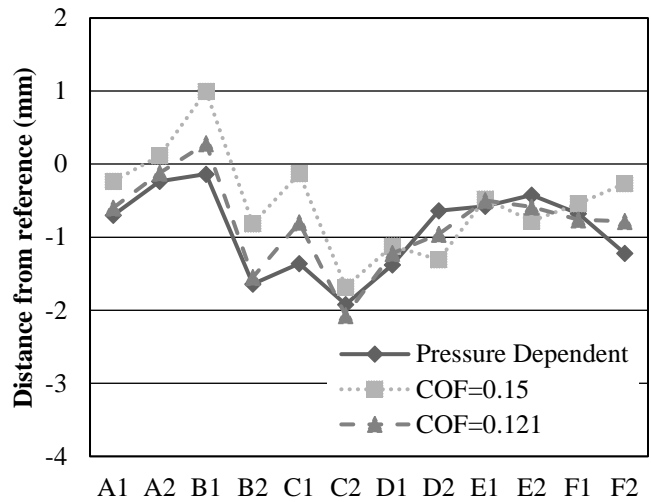
6 Results and discussion

6.1 Effect of COF model on numerical springback prediction

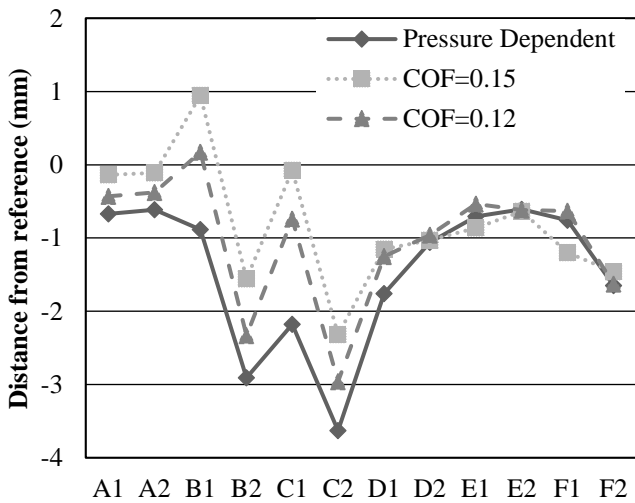
The analysis of the springback was made by measuring the distance between the final simulated geometry and the nominal geometry of the B-Pillar reinforcement on 12 evaluation points. These results are presented in Figure 8.



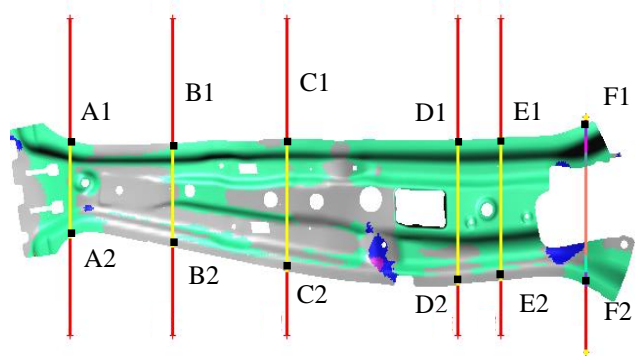
(a)



(b)



(c)



(d)

Figure 8 – Effect of coefficient of friction on springback predictions for a) DX54D, b) HSLA380 and c) DP780 at d) 12 measurement points

It can be seen that DX54D shows similar results with the three COF models. However, HSLA380 and especially DP780 show a greater difference in the results depending on the COF model applied. All the materials show that the pressure dependent model gives as a result the largest elastic recovery.

Figure 9 shows the average distance at the measured points between the final simulated geometry and the nominal geometry. Importantly, the effect of the COF model is different for each material.

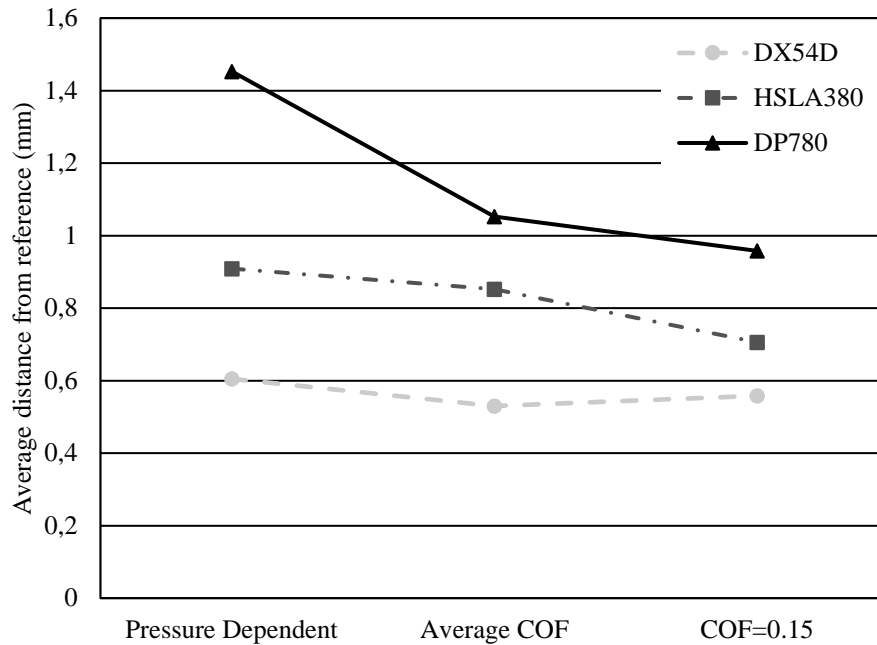


Figure 9 – Average effect of different coefficient of friction models on springback predictions

It can be noted that the DP780 has a difference of 0.5 mm (34%) and 0.4 mm (27%) between defining a pressure dependent COF and a constant COF of 0.15 or the average COF respectively. HSLA380 shows a 0.2 mm (22%) of difference between the pressure dependent and the 0.15 constant COF model, whereas the difference between the variable COF model and the constant average COF values is negligible. In contrast, DX54D shows less variable results using different COF. DX54D is the material with less springback trend and the COF did not show a very variable behavior so the results do not differ too much between the three COF models.

The friction characterization of this study, Section 3, showed that DP780 has the most variable COF with pressure changes. Assuming that high strength materials show a higher springback, the results in Figure 9 state that the COF model definition is critical for this type of materials. However both the DX54D and HSLA380 showed a similar variation of COF with pressure changes but the impact of the pressure dependent COF model was higher on the high strength steel. This fact is because high strength steels are more sensitive to material parameters definition and COF variations for springback predictions due to their high elastic recovery trends. So it can be concluded that the COF model definition is of great relevance for springback predictions of high strength steels. This contradicts previous assumptions made concluding that COF is not an influencing parameter on springback predictions [15].

6.2 Comparison between numerical results and experimental results

The differences between the experimental results and the numerical predictions in terms of final geometry of the component have been calculated using 32 measurement points (defined by the die supplier client). These points are shown in Figure 10. As the experimental work was done with the HSLA380, only the numerical simulations of this material were compared.

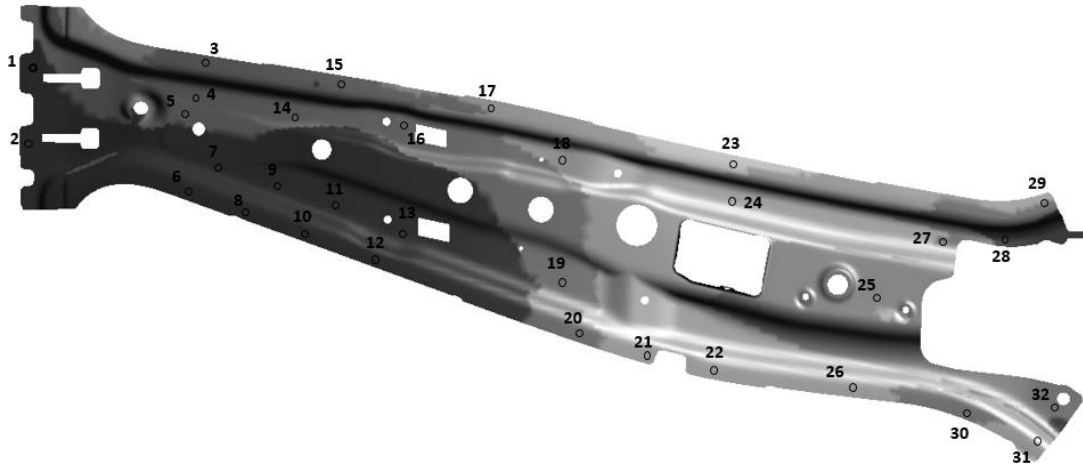


Figure 10 – 32 measurement points to compare numerical results with experimental geometry

Figure 11 shows the percentage of measurement points with an error between experimental measurement and numerical result within $\pm 0,5\text{mm}$ and $\pm 1\text{mm}$. These two ranges of accuracy have been defined based on the automotive sector standard requirements.

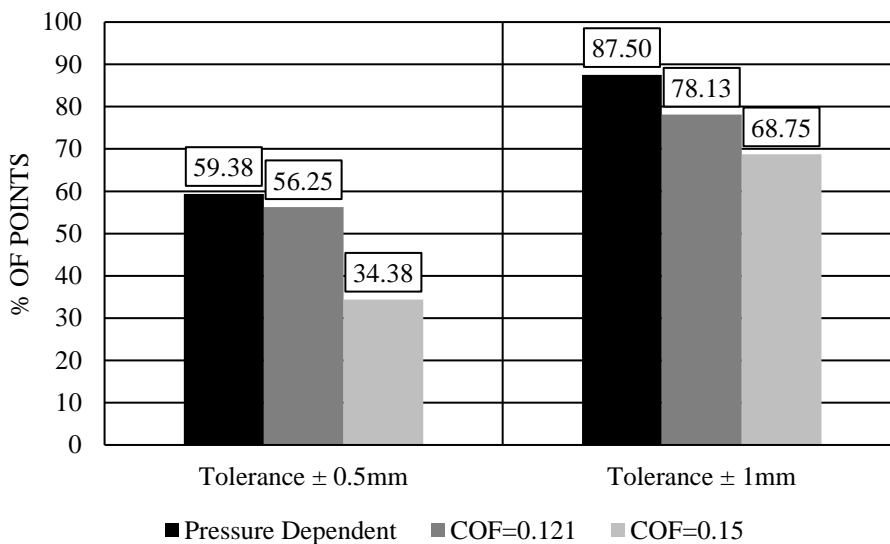


Figure 11 – Percentage of matching rate between numerical simulation models and experimental measurements

The pressure dependent COF model has the highest concordance with the experimental results for both ranges of tolerances. Even if this material did not show a greatly variable COF, it can be seen that the definition of a pressure dependent COF improves the springback prediction when compared to a constant COF model.

7 Conclusions

In this work, Strip Drawing tests were conducted to characterize the COF of a DX54D, a HSLA380 and a DP780 at different contact pressures. Then, different COF models were implemented in a numerical simulation of an industrial B-Pillar reinforcement to evaluate their effect on the springback predictions. Finally, the HSLA380 numerical predictions were compared with an experimental component to evaluate the correlation

between the COF models and the real measurements. The following conclusions were reached:

- All the materials show a decreasing tendency of the COF as the contact pressure increases in a range from 1 to 16 MPa. DP780 is the material that has the most variable COF, a reduction of around 30% from 1 to 16 MPa. It was also observed that DX54D and HSLA380 offer more stable results in terms of COF.
- The results confirmed that the pressure dependent friction model developed by Filzek accurately reproduces the COF tendency for the studied materials with an averaged error lower than 3%.
- The higher the strength of the material is, the more relevant the COF model definition becomes. Pressure dependent COF predicts larger values of springback. For both, HSLA380 and DP780, the effect of defining a pressure dependent or a constant value of COF induces important springback differences. DX54D is not so influenced by the COF model in terms of springback prediction and this can be associated to the weak springback on this material.
- The pressure dependent COF model was the model that best fitted the numerical predictions and the experimental measurements. Compared to the results of a constant COF of 0.12, the pressure dependent model improved the matching rate by 3% and 7% for a tolerance of ± 0.5 mm and ± 1 mm respectively. Compared to the constant COF of 0.15, the improving percentage rises to 25% and 20% in a tolerance of ± 0.5 mm and ± 1 mm respectively.

Acknowledgments

The work presented in this paper has been carried out in cooperation with MATRICI S. Coop. in a research framework that aims at optimizing the forming of Advanced High Strength Steels. The economic support of MATRICI S.Coop is gratefully acknowledged by the authors. The economic support of the Basque Government, through the TRALPRES research project, is also gratefully acknowledged.

References

- [1] Eggertsen P-A, Mattiasson K. Experiences from experimental and numerical springback studies of a semi-industrial forming tool. *Int J Mater Form* 2012;5:341–59. doi:10.1007/s12289-011-1052-9.
- [2] Chen J, Xiao Y, Ding W, Zhu X. Describing the non-saturating cyclic hardening behavior with a newly developed kinematic hardening model and its application in springback prediction of DP sheet metals. *J Mater Process Technol* 2015;215:151–8. doi:10.1016/j.jmatprotec.2014.08.014.
- [3] Eggertsen P a., Mattiasson K. On constitutive modeling for springback analysis. *Int J Mech Sci* 2010;52:804–18. doi:10.1016/j.ijmecsci.2010.01.008.
- [4] Zang SL, Lee MG, Hoon Kim J. Evaluating the significance of hardening behavior and unloading modulus under strain reversal in sheet springback prediction. *Int J Mech Sci* 2013;77:194–204. doi:10.1016/j.ijmecsci.2013.09.033.
- [5] Koc M, Chen P. Simulation of springback variation in forming of advanced high strength steels. *J Mater Process Technol* 2007;190:189–98. doi:10.1016/j.jmatprotec.2007.02.046.
- [6] Wang F, You Y-P. Finite element analysis on influencing factors of springback in sheet

- metal V-bending. *Shenyang Gongye Daxue Xuebao/Journal Shenyang Univ Technol* 2012;34:526–9+535. doi:CNKI:21-1189/T.20120425.1136.006.
- [7] Narayanasamy R, Padmanabhan P. Influence of Lubrication on Springback in Air Bending Process of Interstitial Free Steel Sheet. *J Mater Eng Perform* 2010;19:246–51. doi:10.1007/s11665-009-9479-6.
- [8] Santos AD, Teixeira P. A study on experimental benchmarks and simulation results in sheet metal forming. *J Mater Process Technol* 2008;199:327–36. doi:10.1016/j.jmatprotec.2007.08.039.
- [9] Karupannasamy DK, Hol J, de Rooij MB, Meinders T, Schipper DJ. A friction model for loading and reloading effects in deep drawing processes. *Wear* 2014;318:27–39. doi:10.1016/j.wear.2014.06.011.
- [10] Hol J, Cid Alfaro M V., de Rooij MB, Meinders T. Advanced friction modeling for sheet metal forming. *Wear* 2012;286-287:66–78. doi:10.1016/j.wear.2011.04.004.
- [11] Tamai Y, Inazumi T, Manabe K. FE forming analysis with nonlinear friction coefficient model considering contact pressure, sliding velocity and sliding length. *J Mater Process Technol* 2016;227:161–8. doi:10.1016/j.jmatprotec.2015.08.023.
- [12] Filzek J, Ludwig M, Groche P. Improved FEM Simulation of Sheet Metal Forming with Friction Modelling using Laboratory Tests, IDDRG; 2011.
- [13] Merklein M, Zoeller F, Sturm V. Experimental and numerical investigations on frictional behaviour under consideration of varying tribological conditions. *Adv Mater Res* 2014;966-967:270–8. doi:10.4028/www.scientific.net/AMR.966-967.270.
- [14] Ma X, de Rooij M, Schipper D. A load dependent friction model for fully plastic contact conditions. *Wear* 2010;269:790–6. doi:10.1016/j.wear.2010.08.005.
- [15] Asgari SA, Pereira M, Rolfe BF, Dingle M, Hodgson PD. Statistical analysis of finite element modeling in sheet metal forming and springback analysis. *J Mater Process Technol* 2008;203:129–36. doi:10.1016/j.jmatprotec.2007.09.073.
- [16] Nanu N, Brabie G. Analytical model for prediction of springback parameters in the case of U stretch-bending process as a function of stresses distribution in the sheet thickness. *Int J Mech Sci* 2012;64:11–21. doi:10.1016/j.ijmecsci.2012.08.007.
- [17] de Souza T, Rolfe BF. Understanding robustness of springback in high strength steels. *Int J Mech Sci* 2013;68:236–45. doi:10.1016/j.ijmecsci.2013.01.021.
- [18] Lee J-Y, Barlat F, Lee M-G. Constitutive and friction modeling for accurate springback analysis of advanced high strength steel sheets. *Int J Plast* 2015;71:113–35. doi:10.1016/j.ijplas.2015.04.005.
- [19] Karupannasamy DK, de Rooij MB, Schipper DJ. Multi-scale friction modelling for rough contacts under sliding conditions. *Wear* 2013;308:222–31. doi:10.1016/j.wear.2013.09.012.
- [20] Zhang XK, Zheng GJ, Hu JN, Li CG, Hu P. Compensation factor method for modeling springback of auto parts constructed with high-strength steel. *Int J Automot Technol* 2010;11:721–7.